Sulfate Content and Specific Glycosaminoglycan Backbone of Perlecan Are Critical for Perlecan's Enhancement of Islet Amyloid Polypeptide (Amylin) Fibril Formation

Gerardo M. Castillo, Joel A. Cummings, Wenhua Yang, Martin E. Judge, Malcolm J. Sheardown, Karin Rimvall, John Bondo Hansen, and Alan D. Snow

Islet amyloidosis is characterized by the deposition and accumulation of amylin in pancreatic β-cells and is observed in 90% of patients with type 2 diabetes. Previous studies have also revealed the presence of the specific heparan sulfate proteoglycan, perlecan, colocalized to islet amyloid deposits, similar to perlecan's known involvement with other amyloid proteins. In the present study, perlecan purified from the Engelbreth-Holm-Swarm (EHS) tumor was used to define perlecan's interactions with amylin (i.e., islet amyloid polypeptide) and its effects on amylin fibril formation. Using a solid phase–binding immunoassay, human amylin, but not rat amylin, bound immobilized EHS perlecan with a single dissociation constant (K_d) = 2.75 × 10^{-6} mol/l. The binding of human amylin to perlecan was similarly observed using perlecan heparan sulfate glycosaminoglycans (GAGs), and was completely abolished by 10 μmol/l heparin. Using thioflavin T fluorometry, Congo red staining, and electron microscopy methodology, intact perlecan was found to enhance amylin fibril formation in a dosage-dependent manner, with the majority of these effects attributed to the heparan sulfate GAG chains of perlecan. Other sulfated GAGs and related macromolecules were also effective in the enhancement of amylin fibril formation in the order of heparin > heparan sulfate > chondroitin-4-sulfate = dermatan sulfate = dextran sulfate > pentosan polysulfate, implicating the importance of the specific GAG/carbohydrate backbone. The sulfate content of heparin/heparan sulfate was also important for the enhancement of amylin fibril formation in the order of heparin > *N*-desulfated *N*-acetylated heparin > completely desulfated *N*-sulfated heparin > completely desulfated *N*-acetylated heparin. These studies suggest that the enhancement effects of perlecan on amylin fibril formation are mediated primarily by both specific GAG chain backbone and GAG sulfate content, and implicate perlecan as an important macromolecule that is likely involved in the pathogenesis of islet amyloidosis. *Diabetes* 47:612–620, 1998

Type 2 diabetes is characterized by insulin resistance, impaired glucose tolerance, and the presence of amyloid deposits in the pancreatic islets of ~90% of patients (1,2). The major protein in the islet amyloid is a 37–amino acid peptide termed islet amyloid polypeptide or amylin (3), a known normal secretory product of the pancreatic β-cells (4) that is stored in insulin-bearing cytoplasmic granules (5). Fibrillar amylin deposition is believed to lead to the progressive deterioration of β-cell function, as observed in vitro (6,7) and in vivo (8,9). Overexpression of human amylin (but not rat amylin) can result in amyloid formation that is believed to contribute to cell death (10). Human amylin fibrils are toxic to insulin-producing β-cells of the adult pancreas in both humans and rats (6). The mechanism of cell death involves RNA and protein synthesis and is characterized by plasma membrane blebbing, chromatin condensation, and DNA fragmentation, indicating that amylin induces islet cell apoptosis (6). These findings indicate that amylin fibril formation in the pancreas may cause islet cell dysfunction and cell death in type 2 diabetes.

Fibrillar amylin deposition in the islets of Langerhans of type 2 diabetic patients is also known to be associated with the accumulation of a specific heparan sulfate proteoglycan, known as perlecan. Young et al. (11) previously demonstrated the specific co-localization of perlecan immunoreactivity to islet amyloid deposits in the pancreas of type 2 diabetic patients, and more recent studies by others have demonstrated the accumulation of perlecan in islet amyloid deposits of transgenic mice that overexpressed amylin and developed hyperglycemia (12,13). Perlecan has been postulated to play a primary role in most, if not all, forms of amyloidosis (14). Consistent with this hypothesis, perlecan specifically co-localizes to the β-amyloid (Aβ) protein–containing amyloid deposits of Alzheimer's disease (15–19) and Down's syndrome (16), the amyloid fibrils in the prion protein–containing amyloid plaques of the prion diseases (i.e., Creutzfeldt-Jakob disease, Gerstmann-Straussler syndrome, and kuru) (20), and the AA amyloid protein of inflammation-associated amyloidosis (21). The constant presence of perlecan in a variety of

From the Department of Pathology (G.M.C., J.A.C., W.Y., A.D.S.), University of Washington, Seattle, Washington; and Novo Nordisk (M.E.J., M.J.S., K.R., J.B.H.), Health Care Discovery, Malov, Denmark.

Address correspondence and reprint requests to Dr. Alan Snow, University of Washington, Department of Pathology, Neuropathology Laboratories Box 356480, Seattle, WA 98195-6480. E-mail: asnow@u.washington.edu.

Received for publication 25 June 1997 and accepted in revised form 24 December 1997.

Aβ, β-amyloid protein; BSA, bovine serum albumin; EHS, Engelbreth-Holm-Swarm; GAG, glycosaminoglycan; K_d, dissociation constant; M_r, molecular weight; OD, optical density; TBS, Tris-buffered saline; TTBS, TBS containing 100 mmol/l Tris-HCl, 50 mmol/l NaCl, 0.05% Tween-20, and 3 mmol/l NaN_3.

different amyloids, regardless of the nature of the underlying amyloid protein and the extent of amyloid deposition, suggests that perlecan represents a common component that may play important roles in amyloidogenesis.

In the present study, perlecan purified from the Engelbreth-Holm-Swarm (EHS) tumor (22) was used to test the hypotheses that *1*) other amyloid proteins (e.g., amylin) also specifically interact with perlecan, and *2*) perlecan enhances amylin fibril formation in a manner similar to that recently observed with the Aβ of Alzheimer's disease (23,24). The results of the present study, in which solid phase–binding immunoassay, thioflavin T fluorometry, Congo red staining, and electron microscopy were used, indicated that both sulfate content and specific glycosaminoglycan (GAG) backbone of heparan sulfate and perlecan GAGs (which contain heparan sulfate) are critical structural elements that participate in the enhancement of amylin fibrillogenesis.

RESEARCH DESIGN AND METHODS

Perlecan isolation from the EHS tumor. Perlecan used in the present study was purified from the EHS tumor, as previously described (22). The final purity and quality of the perlecan preparations were assessed by Alcian blue staining, Coomassie Blue staining, silver staining, and a series of Western blots using antibodies against perlecan, laminin, type IV collagen, and fibronectin, as described (22).

Solid phase–binding immunoassay studies. To determine the amount of perlecan bound to microtiter wells, perlecan was first labeled with ^{125}I using Iodobeads (Pierce, Rockford, IL) according to the manufacturer's protocol. ^{125}I-perlecan was diluted with unlabeled perlecan to reach 3,500 dpm/μg. Aliquots of perlecan (0.5 or 1 μg in 40 μl Tris-buffered saline [TBS]; pH 7.4) were then allowed to bind overnight to microtiter wells (Maxisorb; Nunc, Naperville, IL) at 4°C. The supernatants were removed and the wells were washed twice with TBS containing 100 mmol/l Tris-HCl, 50 mmol/l NaCl, 0.05% Tween-20, and 3 mmol/l NaN_3 (pH 7.4) (TTBS) plus 2% bovine serum albumin (BSA). The supernatants from the two washes were then pooled, and the radioactivity was determined using a gamma counter. The amount of bound perlecan was calculated as the total dpm minus the unbound dpm. It was determined that of 1 and 0.5 μg of perlecan, 0.27 μg (27%) and 0.07 μg (14%) of perlecan bound, respectively. Using this information, a series of solid phase–binding immunoassay studies were performed to determine the binding affinities of amylin to perlecan under various conditions. For these studies, aliquots of perlecan (0.5 or 1 μg in 40 μl TBS; pH 7.4) were allowed to bind overnight to microtiter wells at 4°C. All of the microtiter wells (including blank wells without perlecan) were blocked by incubating with 300 μl TTBS and 2% BSA for 2 h (pH 7.4) followed by five rinses with TTBS. Various dilutions (0.005–2,000 $\times 10^{-9}$ mol/l) of freshly aliquoted human amylin (Lot #WL934; Bachem, Torrance, CA) or rat amylin (Lot #033529; Peninsula Labs, Belmont, CA) in 250 μl of TBS (pH 7.4) were placed in wells (in triplicate) containing either substrate-bound perlecan or blank and were allowed to bind overnight at 4°C. In addition, binding of human amylin to substrate-bound EHS perlecan was assessed in the presence or absence of 10 μmol/l heparin (based on an average molecular weight [M_r] of 6 kDa) (porcine intestinal mucosal heparin; Sigma, St. Louis, MO). The next day, unbound amylin was washed three times with TTBS; then 100 μl (1:1,000 in TTBS) of anti-amylin antibody (Chemicon, Temicula, CA; mouse monoclonal antibody that recognizes both human and rat amylin residues 29–37) was aliquoted and incubated for 1.5 h on a rotary shaker at room temperature. After washing three times with TTBS, the amount of bound amylin was detected after incubation with 100 μl (1:500 dilution) of biotinylated goat anti-mouse and peroxidase-avidin complex (1:250 dilution) in TTBS with 0.1% BSA for 1 h on a rotary shaker. The wells were then rinsed three times with TTBS, and 100 μl of a substrate solution (OPD-Sigma Fast; Sigma, St. Louis, MO) was added to each well and allowed to develop for 5 min. The reaction was stopped with 50 μl of 4 N H_2SO_4 and read on a Model 450 microplate reader (Biorad, Hercules, CA) at 490 nm. Data points representing mean of triplicate determination were plotted (minus background and nonspecific binding), and the dissociation constants (i.e., K_d) were determined using Ultrafit (version 2.1; Biosoft, Cambridge, U.K.), as described below.

Isolation of EHS perlecan GAG chains. The ability of heparan sulfate GAG chains isolated from perlecan to bind amylin and their effects on amylin fibril formation were also assessed. Isolation of perlecan GAG chains by alkaline borohydride treatment was performed as described previously (25). Briefly, 1 mg of lyophilized perlecan was dissolved in 100 μl of 0.2 mol/l NaOH · 1 mol/l $NaBH_4$ and incubated for 2 days at room temperature. After neutralization with 15 μl of 2 mol/l acetic acid, the perlecan GAGs were precipitated with 5 vol of absolute ethanol and dissolved in 7 mol/l urea buffer as described above. GAGs were then bound to a 0.5 ml DEAE-Sephacel column equilibrated with urea buffer and then washed with 5 vol of urea buffer to remove further traces of proteins that may have survived the alkaline borohydride treatment. Perlecan GAGs were eluted from the DEAE-Sephacel column with 5 vol of urea buffer containing 3 mol/l NaCl followed by precipitation with 5 vol of absolute methanol (25). The concentration of GAGs was determined using an Alcian blue assay (26). For the solid phase–binding immunoassay studies, an initial pilot experiment determined that when 4 μg of perlecan GAGs in 40 μl TBS were incubated in microtiter wells overnight at 4°C, 0.21 μg (5.25%) bound to each well.

Analysis of amylin fibrillogenesis by thioflavin T fluorometry, Congo red staining, and electron microscopy. The effects of intact perlecan, perlecan GAGs, other types of GAGs (or related carbohydrates), and modified heparins on amylin fibrillogenesis were also determined using the previously described method of thioflavin T fluorometry (27–30). For these studies, 25 μmol/l of amylin was incubated in microcentrifuge tubes at 37°C for 1 week (in triplicate) either alone or in the presence of increasing concentrations of perlecan (32, 48, 64, 80, or 96 μg/ml) or perlecan GAGs (32, 48, 64, 80, or 96 μg/ml), heparin (100 μg/ml; porcine intestinal mucosa; Sigma), heparan sulfate (100 μg/ml; kidney; Sigma), chondroitin 4-sulfate (100 μg/ml; porcine rib; Sigma), dermatan sulfate (100 μg/ml; bovine intestinal mucosa; Sigma), dextran sulfate (100 μg/ml; M_r = 8 kDa; Sigma), pentosan polysulfate (100 μg/ml; Sigma), *N*-desulfated *N*-acetylated heparin (100 μg/ml; Seikagaku, Rockville, MD), completely desulfated *N*-sulfated heparin (100 μg/ml; Seikagaku), or completely desulfated *N*-acetylated heparin (100 μg/ml; Seikagaku) in 100 mmol/l Tris-HCl, 50 mmol/l NaCl (pH 7.0; TBS). Aliquots (50 μl) were then taken from each tube for analysis at 1 h, 1 day, 3 days, and 1 week. The 50 μl aliquots were added to 1.2 ml thioflavin T reagent containing 100 μmol/l thioflavin T (Aldrich) and 50 mmol/l $NaPO_4$ (pH 6.0). The use of thioflavin T at 100 μmol/l was determined to have a linear fluorescence response with increasing amylin concentrations (not shown), indicating an absence of any possible disproportionate inner filter effects. Fluorescence emission at 480 nm was measured on a Turner Model 450 fluorometer (Biomolecular, Reno, NV) at an excitation wavelength of 450 nm. For each determination, the fluorometer was calibrated by zeroing in on the presence of the thioflavin T reagent alone, and by setting the 50 ng/ml riboflavin (Sigma) in the thioflavin T reagent to 1,800 fluorescence units. All fluorescence determinations were based on these references, and any fluorescence given off by any of the compounds in the presence of the thioflavin T reagent was subtracted from all pertinent readings. Aliquots (10 μl) of mixtures containing amylin only, perlecan alone, or amylin plus perlecan that had been incubated for 1 h were also taken, allowed to air dry on gelatin-coated slides, and Congo red stained (31).

Furthermore, aliquots of mixtures of amylin only, amylin plus perlecan, or amylin plus perlecan GAGs that had been incubated for 1 h were taken for analysis using negative-stain electron microscopy. For these studies, microscopy was performed by floating pioloform, carbon-coated grids on the various solutions, which were then blotted and stained with 1% phosphotungstic acid. Preparations were visualized on a JOEL 100B electron microscope (Tokyo, Japan) operated at 60 kV.

Quantitative analysis of binding data. The binding data were analyzed assuming a thermodynamic equilibrium for the formation of the complex (B-L) from the amylin ligand in solution (L) and the uncomplexed perlecan adsorbed to the microtiter well (B) according to the equation $K_d = [B] \times [L] / [B\text{-}L]$. The K_ds were determined using an enzyme-linked immunoassay that gives a color signal that is proportional to the amount of unmodified amylin bound to perlecan or perlecan GAGs (32–34). Identical K_ds were obtained when different amounts of perlecan or perlecan GAGs were bound to the plate, indicating accurate determinations as previously described (32–34).

To account for potential nonspecific binding, control wells without perlecan (in triplicate) were included for each concentration of amylin used in each binding experiment. Optical densities (ODs) of the control wells never exceeded 0.05 at all amylin concentrations used in these experiments. The ODs of the control wells were subtracted from the ODs of the perlecan-containing wells that received similar amylin concentrations. Nonspecific absorbance obtained from perlecan-containing wells that did not received amylin were also subtracted from all data points. Thus the equation $OD_{exp} = OD_o + [S \times (amylin)] + \{OD_{max} \times [amylin]/[(amylin) + K_d]\}$, where $[S \times (amylin)]$ represents the nonspecific binding (control wells) and OD_o is the nonspecific absorbance, becomes $OD_{exp} = OD_{max} \times [amylin]/[(amylin) + K_d]$. Therefore, at 50% saturation, $OD_{exp} = 0.50\ OD_{max}$ and K_d = (amylin). Determinations of (amylin) at 50% saturation were performed by nonlinear least square program (Ultrafit; Biosoft, Cambridge, U.K.) using a one-site model.

RESULTS

Binding of human (but not rat) amylin to immobilized EHS perlecan. Previous studies have demonstrated that human amylin spontaneously forms amyloid fibrils, whereas rat amylin does not (due to the five amino acid differences

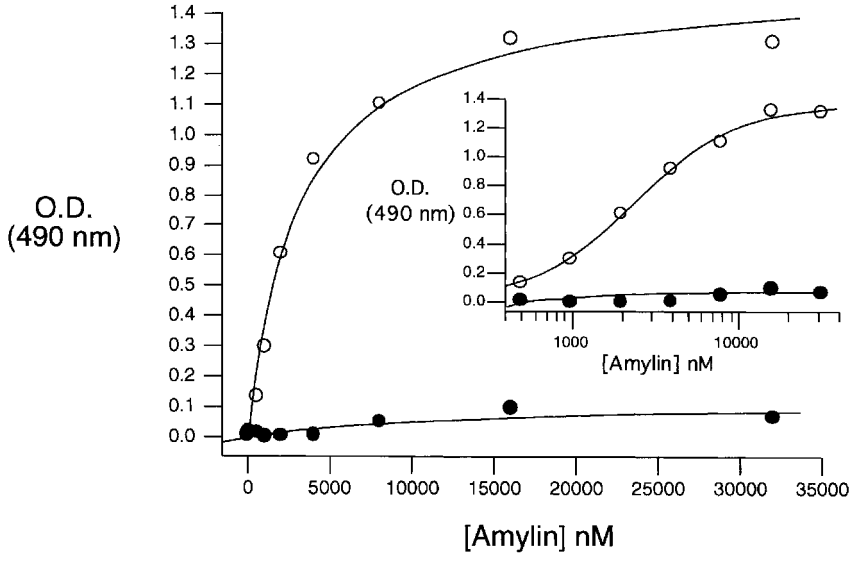

FIG. 1. Binding of human versus rat amylin to immobilized perlecan. A solid phase–binding immunoassay was used to compare the binding of human versus rat amylin to immobilized EHS perlecan. Bound amylin was detected using anti-amylin antibodies (mouse monoclonal antibody, which recognizes both human and rat amylin 29–37). Data points representing the mean of triplicate determinations were plotted and the dissociation constant (K_d) determined using the Ultrafit program. Shown is the relative amount (OD 490 nm) of human amylin (○) versus rat amylin (●), bound to immobilized perlecan as a function of amylin concentration. The inset is a semilogarithmic plot of the same data revealing a single K_d (2.0×10^{-6} mol/l) for human amylin. No interaction of rat amylin with perlecan was observed.

between human and rat amylin within residues 20–29) (35). Initial experiments determined whether *1*) human amylin bound immobilized perlecan and *2*) differences existed in human versus rat amylin binding to perlecan. As shown in Fig. 1, using a solid phase–binding immunoassay, human amylin bound immobilized EHS perlecan with a single K_d (Fig. 1, ○), whereas rat amylin did not bind (Fig. 1, ●). Human amylin bound EHS perlecan in a concentration dependent and saturable manner with a $K_d = 2.0 \times 10^{-6}$ mol/l (Fig. 1). The concentration of human amylin at 50% saturation did not change, even when the amount of perlecan bound to the plate was changed (not shown), indicating an accurate K_d determination (32–34). The apparent dissociation constant described above was based on human amylin having a M_r of ~3.7 kDa. However, it was clear from the thioflavin T (Fig. 4) and Congo red staining data (Fig. 5) that amylin fibrils had formed even after a 1-h incubation. Therefore, the apparent dissociation constant described above based on human amylin having a M_r of ~3.7 kDa was likely overestimated. Assuming the amyloid fibrils formed contained amylin in a multimeric form with a total M_r of ⩾3.7 kDa, the actual dissociation constant for human amylin binding to EHS perlecan was most likely much lower than described above, in the range of 10^{-9} mol/l.

Amylin binding to perlecan is primarily mediated by perlecan GAGs. To determine whether the heparan sulfate GAG chains of perlecan were primarily responsible for perlecan interactions with amylin, the binding of amylin to intact perlecan versus perlecan GAGs (isolated by alkaline borohydride treatment) was directly compared. As shown in Fig. 2, perlecan GAGs bound amylin in an almost identical manner to that observed with intact perlecan. The binding of amylin to intact perlecan (Fig. 2, ●) had an apparent $K_d = 2.7 \times 10^{-6}$ mol/l, whereas the binding of amylin to perlecan GAGs (Fig. 2, ○) had an apparent $K_d = 2.8 \times 10^{-6}$ mol/l.

To further confirm the specificity of the binding of perlecan heparan sulfate GAGs to amylin, the binding of amylin to intact perlecan in the presence or absence of heparin was determined. As shown in Fig. 3, heparin at 10 µmol/l completely blocked the binding of human amylin to perlecan. Because heparin has a somewhat similar structure to heparan sulfate (36), these data also suggested that *1*) the binding of perlecan to amylin was primarily mediated via the heparan sulfate GAG chains of perlecan, and *2*) heparin can bind to the site in amylin responsible for perlecan binding.

Perlecan enhances amylin fibril formation in a dosage-dependent manner. To determine the possible effects of perlecan and perlecan heparan sulfate GAGs on amylin fibril formation, a thioflavin T fluorometric assay was used (27–30). In a first set of studies, the effects of increasing concentrations of perlecan (Fig. 4*A*) on amylin fibril formation were evaluated over 1 week. Freshly solubilized amylin (25 µmol/l) was already in a fibrillar form, reaching a maximum fluorescence at 1-h incubation that did not significantly change over the 1-week experimental period (Fig. 4), primarily due to the establishment of an equilibrium (i.e., between monomeric and fibrillar amylin) from the onset. Increasing concentrations of perlecan (32, 48, 64, 80, and 96 µg/ml) enhanced amylin fibril formation in a dosage-dependent manner at all time points, as shown by progressively increasing thioflavin T fluorescence (Fig. 4*A*). Perlecan's effects on amylin fibril formation were significant ($P < 0.005$) at concentrations of ≥64 µg/ml at all time points during the 1-week incubation period. At 1 week, 96 µg/ml of perlecan caused a 1.8-fold increase in amylin fibril formation, as indicated by thioflavin T fluorescence (Fig. 4*A*).

Perlecan GAGs (Fig. 4*B*) also enhanced amylin fibril formation in a similar dosage-dependent manner as observed with intact perlecan. At all time points during the 1-week incubation period, perlecan GAG's ability to enhance amylin fibril formation was significant ($P < 0.005$) at concentrations ≥32 µg/ml. At 1 week, 96 µg/ml of perlecan GAGs caused a 3-fold increase in amylin fibril formation (Fig. 4*B*). These studies indicated that the enhancement of amylin fibril formation by perlecan was primarily attributed to the heparan sulfate GAG chains of perlecan.

Congo red staining of human amylin (25 µmol/l) in the absence or presence of perlecan (i.e., 100 µg/ml) was also assessed at various time points during the 1-week incubation period to determine whether perlecan caused a correlative increase in the extent of amylin fibrillogenesis, as demonstrated by enhancement of Congo red staining. Figure 5 demonstrates the Congo red staining of human amylin in the absence (Fig. 5*A* and *B*) or presence of perlecan (Fig. 5*C* and *D*) after a

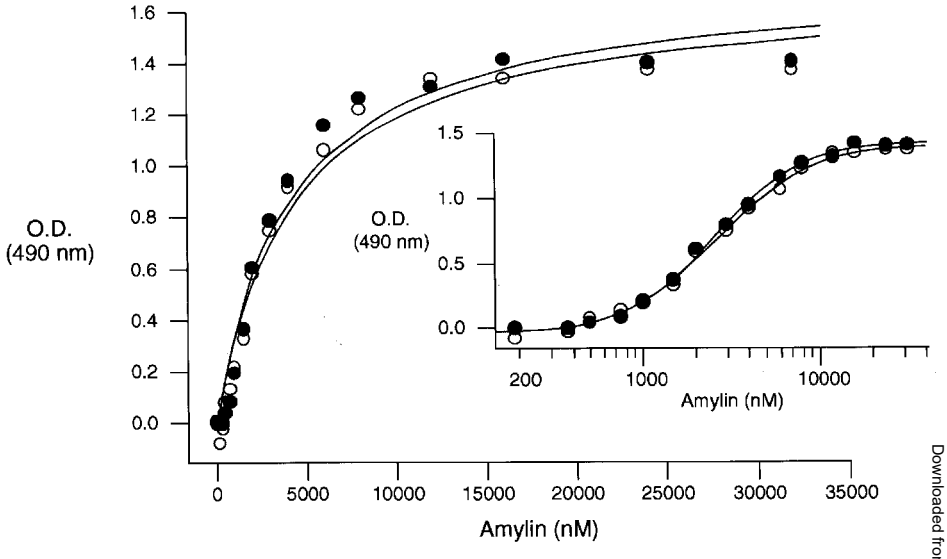

FIG. 2. Binding of human amylin to immobilized perlecan heparan sulfate GAGs. A solid phase–binding immunoassay was used to compare the binding of human amylin to immobilized EHS perlecan versus perlecan heparan sulfate GAGs. Data points representing the mean of triplicate determinations were plotted and the dissociation constants (K_ds) determined using the Ultrafit program. Shown is the relative amount (OD 490 nm) of human amylin bound to immobilized EHS perlecan (●) in comparison with perlecan GAGs (○) as a function of amylin concentration. The inset is a semilogarithmic plot of the same data. Human amylin bound perlecan heparan sulfate GAGs (K_d = 2.8 × 10^{-6} mol/l) in an almost identical manner to that observed with intact perlecan (K_d = 2.7 × 10^{-6} mol/l).

1-h incubation. Congo red staining of amylin alone demonstrated positive staining (i.e., classic red/green birefringence as viewed under polarized light and indicative of amyloid) (31) throughout a 10-µl air-dried aliquot, which was primarily noticeable at the periphery (Fig. 5*A* and *C*, *arrowhead*), similar to that previously observed (37). In comparison, a 1-h incubation of perlecan with amylin resulted in a marked contraction of the fibrillar material, which correlated with an apparent qualitative increase in the amount of amylin fibrils formed (compare Fig. 5*C* vs. 5*A*). The increase in Congo red–stained material caused by perlecan (Fig. 5*C* and *D*) correlated with perlecan's ability to enhance amylin fibril formation, demonstrated by the thioflavin T fluorescence data presented above (Fig. 4).

Electron microscopic analysis (using negative staining) confirmed the results observed at the light microscopic level using Congo red staining. After a 1-h incubation, amylin alone demonstrated the presence of amyloid fibrils with a fibril diameter of 7–10 nm (Fig. 6*A*, *arrows*). Perlecan alone demonstrated coalescing globular structures (Fig. 6*B*, *arrows*) indicative of perlecan's globular domains. Perlecan plus amylin demonstrated a qualitative increase in amyloid fibrils and a general compaction of the fibrils (Fig. 6*C*). A similar compaction of fibrils was observed when amylin was incubated with heparin (Fig. 6*D*).

Enhancement of amylin fibril formation by other sulfated GAGs and related sulfated macromolecules. Because the heparan sulfate GAGs of perlecan appear to be primarily responsible for perlecan's enhancement of amylin fibril formation, the next study tested other sulfated GAGs (including heparin, heparan sulfate from kidney, chondroitin-4-sulfate, and dermatan sulfate) and related sulfated macromolecules (including dextran sulfate and pentosan polysulfate) on a per weight basis (i.e., 100 µg/ml) for their ability to enhance amylin fibril formation. As shown in Fig. 7, heparin was the most effective sulfated GAG for enhancement of amylin fibril formation, causing significant (P < 0.005) 2.8-, 3.2-, and 3.9-fold increases at 1 h, 1 day, and both 3 days and 1 week, respectively, compared with amylin alone. This was

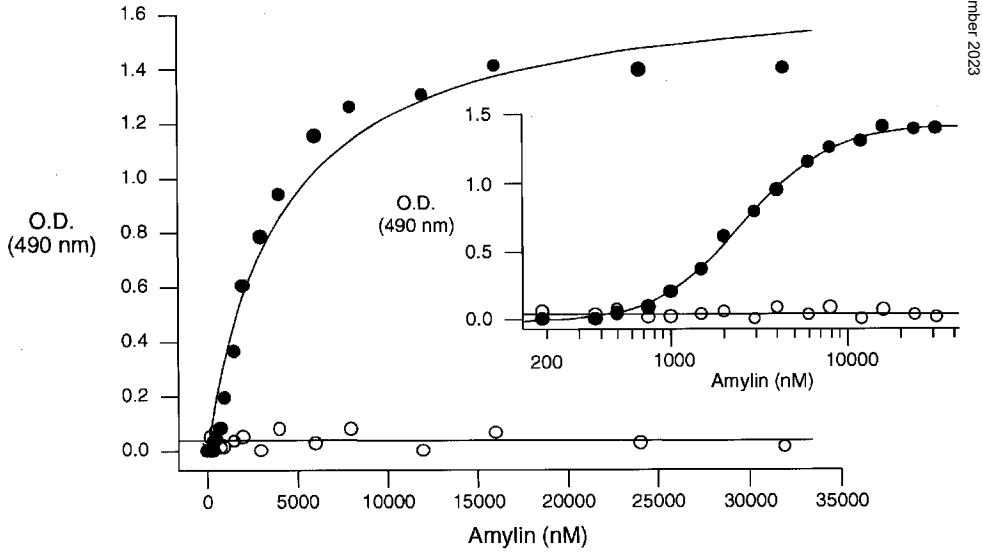

FIG. 3. Inhibition of amylin binding to immobilized perlecan by heparin. A solid phase–binding immunoassay was used to determine the effects of 10 µmol/l heparin on human amylin binding to immobilized EHS perlecan. Data points representing the mean of triplicate determinations were plotted. Shown is the relative amount of human amylin (OD 490 nm) bound to immobilized EHS perlecan in the absence (●) or presence of heparin (○). The inset is a semilogarithmic plot of the same data. Heparin completely blocked the binding of amylin to perlecan.

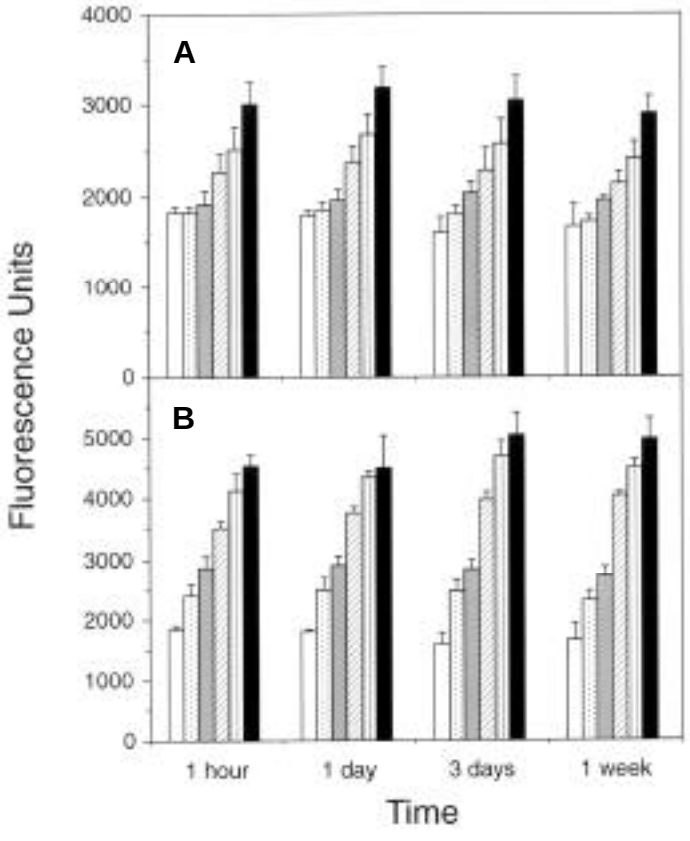

FIG. 4. Dosage-dependent increase in amylin fibril formation in the presence of perlecan or perlecan heparan sulfate GAGs. Amylin (25 µmol/l) was incubated in triplicate at 37°C for 1 week alone (□), or in the presence of 32 (▨), 48 (▩), 64 (▨), 80 (▥), or 96 (■) µg/ml of perlecan (*A*) or perlecan GAGs (*B*). Aliquots (50 µl) were taken from each tube for thioflavin T fluorometry analysis at 1 h, 1 day, 3 days, and 1 week. Amylin spontaneously formed abundant amyloid fibrils, reaching a maximum fluorescence at 1 h. Both intact perlecan (*A*) and perlecan GAGs (*B*) caused a dosage-dependent increase in the amount of amylin fibrils, as demonstrated by significant increases in thioflavin T fluorescence. The minimum amount of intact perlecan that significantly increased ($P < 0.005$) amylin fibril formation (compared with amylin alone) at all time points was 64 µg/ml (*A*), whereas the minimum amount of perlecan GAGs that significantly increased ($P < 0.005$) amylin fibril formation at all time points was 32 µg/ml (*B*).

followed by heparan sulfate, which was equally as effective as heparin at 1 h and 1 day, and only slightly less effective than heparin at 3 days and 1 week ($P < 0.005$). Chondroitin 4-sulfate was also effective in increasing amylin fibril formation, but less so than heparin or heparan sulfate, causing 2.5-, 2.8-, 3.2-, and 3.0-fold increases at 1 h, 1 day, 3 days, and 1 week, respectively (Fig. 7). The effects of chondroitin-4-sulfate on amylin fibril formation were significantly less ($P < 0.025$) than that observed with heparin at all time points. Both dermatan sulfate and dextran sulfate showed an enhancement of amylin fibril formation similar to that of chondroitin-4-sulfate, causing 2.4- and 3.0-fold increases at 1 h and 1 week, respectively. Of all the GAGs and sulfated macromolecules tested, pentosan polysulfate had the least enhancing effect on amylin fibril formation, causing 2.1-, 1.8-, 2.4-, and 2.2-fold increases at 1 h, 1 day, 3 days, and 1 week, respectively. In summary, all of the sulfated GAGs and related sulfated macromolecules were able to enhance amylin fibril formation (all $P < 0.005$) in the order of heparin > heparan sulfate > chondroitin-4-sulfate = dermatan sulfate = dextran sulfate > pentosan polysulfate. Despite the higher sulfate content of both dextran sulfate and pentosan polysulfate (Table 1), heparin and heparan sulfate were still the most effective enhancers of fibril formation, suggesting that the heparin/heparan sulfate GAG chain backbone was likely partially responsible for the observed effects.

The sulfate content of GAGs is partially responsible for enhancement of amylin fibril formation. To determine whether the sulfate content of GAGs is also partially responsible for the observed effects of increased amylin fibril formation, heparins modified at various positions on the GAG chains were compared with intact heparin and heparan sulfate for their ability to enhance amylin fibril formation (Fig. 8). As previously observed (Fig. 7), 100 µg/ml of heparin (from porcine intestinal mucosa) or heparan sulfate (from bovine kidney) when co-incubated with 25 µmol/l of amylin significantly ($P < 0.005$) increased amylin fibril formation at all time points, causing a 2.9-fold enhancement at 1 h (for both heparin and heparan sulfate), and a 3.9-fold (for heparin) and 3.3-fold (for heparan sulfate) enhancement at 1 week. The enhancement of amylin fibril formation by heparan sulfate was significantly less ($P < 0.005$) than that of heparin at 3 days and 1 week, consistent with heparan sulfate's having an average sulfate content less than that of heparin (averages of ~0.5–0.9 vs. ~2.4 sulfate groups per disaccharide unit, respectively) (38–40). The importance of the sulfate moieties for enhancement of amylin fibril formation was confirmed when 100 µg/ml of *N*-desulfated *N*-acetylated heparin (i.e., removal of *N*-sulfates) increased amylin fibril formation by only 1.9-fold at 1 h and 2.2-fold at 1 week, significantly less ($P < 0.005$) than either heparin or heparan sulfate at all time points (Fig. 8). In comparison with heparin, a similar significant ($P < 0.005$) decrease in the enhancement of amylin fibril formation was observed at all time points using a modified heparin that was completely desulfated *N*-sulfated (i.e., had *O*-sulfates removed), causing only a 1.6-fold increase in amylin fibril formation at 1 h and a 1.8-fold increase at 1 week. *N*-desulfated *N*-acetylated heparin was significantly ($P < 0.05$) more effective in the enhancement of amylin fibril formation than completely desulfated *N*-sulfated heparin at 1 week, suggesting that sulfates in the *O*-position may be more important for enhancement of amylin fibril formation than sulfates in the *N*-position. Heparin that was completely desulfated *N*-acetylated (i.e., had all sulfates removed) was the least effective in enhancing amylin fibril formation, causing only a 1.2-fold increase at 1 h and a 1.5-fold increase at 1 week, in comparison with amylin alone (Fig. 8). In summary, the order of effectiveness for enhancement of amylin fibril formation was heparin/heparan sulfate ⩾ heparin modified by *N*-desulfation *N*-acetylation > heparin modified by complete desulfation *N*-sulfation ⩾ heparin modified by complete desulfation *N*-acetylation. The carboxyl groups of the GAG chains were also believed to play a small but significant role in the enhancement of amylin fibril formation, as complete desulfation and *N*-acetylation still caused a significant ($P < 0.005$) increase in amylin fibril formation compared with amylin alone at all time points studied (Fig. 8).

DISCUSSION

The major findings in the present study were *1*) amylin bound

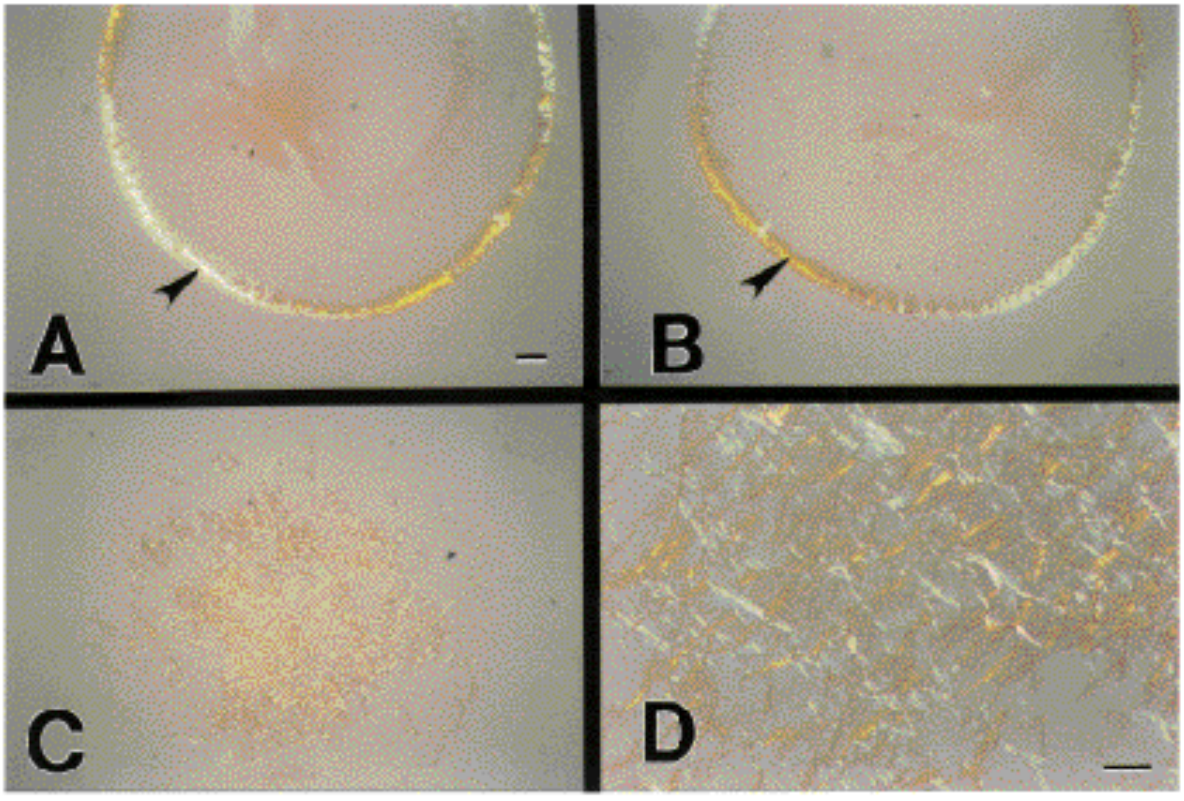

FIG. 5. Congo red staining of amylin fibrils in the absence or presence of perlecan. Aliquots (10 µl) of amylin (25 µmol/l) only (*A* and *B*) or amylin (25 µmol/l) plus perlecan (100 µg/ml) (*C* and *D*) were taken after 1 h of incubation (37°C), air-dried overnight, and stained with Congo red (31). *A* and *B* represent two separate amylin preparations. Congo red staining of amylin air-dried aliquots demonstrated the classic red-green birefringence (as viewed under polarized light), primarily at the periphery of the air-dried aliquots (*arrowhead*, *A* and *B*). Perlecan plus amylin formed condensed fibrils (*C* and *D*) that were much more prominent in comparison with amylin alone. *A–C* were taken at the same magnification, whereas *D* was taken at a higher magnification (bar = 100 µm).

immobilized EHS perlecan with a single dissociation constant, $K_d = 2.6 \times 10^{-6}$mol/l, *2*) perlecan was a potent enhancer of amylin fibril formation in a dosage-dependent manner, and *3*) perlecan's effects on amylin binding and enhancement of amylin fibril formation were mediated primarily by perlecan's heparan sulfate GAG chains. In addition, the present study demonstrated that both the sulfate content and the specific GAG chain backbone were critical for the observed effects of perlecan enhancement of amylin fibril formation.

The roles of GAG sulfate content and specific carbohydrate backbone in the enhancement of amylin fibril formation. The present study demonstrated that other sulfated GAGs and sulfated macromolecules were also capable of enhancing amylin fibril formation in the order of heparin > heparan sulfate > chondroitin-4-sulfate = dermatan sulfate = dextran sulfate > pentosan sulfate. The order of effectiveness suggests that the specific GAG chain backbone may be partially responsible for the enhancement of amylin fibril formation, since highly sulfated carbohydrate non-GAG backbones (such as dextran sulfate and pentosan sulfate, which both contain three to four sulfates per repeating unit) (Table 1) were much less effective enhancers of amylin fibril formation than chondroitin-4-sulfate or dermatan sulfate (which contain a GAG backbone with 1–1.5 sulfates per repeating disaccharide unit) (40,41) . On the other hand, the sulfate content of the specific GAG chain backbone was also partially responsible for the enhancement effects observed, since heparin, which usually contains an average of ~2.4 sulfates per repeating disaccharide unit (see Table 1), had a greater enhancing effect on amylin fibril formation than heparan sulfate, which usually contains an average of 0.5–0.9 sulfates per repeating disaccharide unit (38–40). Consistent with the latter idea of a sulfate-dependent effect, the present study demonstrated that removal of specific sulfate residues in heparin led to correlative decreases in amylin fibril–enhancing activity. For example, completely desulfated *N*-acetylated heparin was a much weaker enhancer of amylin fibril formation compared with heparin or heparan sulfate. In addition, *O*-sulfate appeared to have a greater effect on amylin fibril–enhancing activity than did *N*-sulfate, since *N*-desulfated *N*-acetylated heparin led to a greater amylin-enhancing ability than completely desulfated *N*-sulfated heparin. Therefore, the results of the present study suggest that both GAG chain backbone and sulfate content contribute to the observed enhancement effects of perlecan and perlecan GAGs on amylin fibril formation.

The postulated effects of amylin in type 2 diabetes and the potential role of perlecan. Human amylin is amyloidogenic (35), but despite amylin's presence in pancreatic islet cells and plasma of normal people, 90% of type 2 diabetic individuals demonstrate amyloid deposition in their pancreas. In addition, dogs and cats have identical amyloidogenic amylin sequences, but only cats acquire islet amyloid (42). These

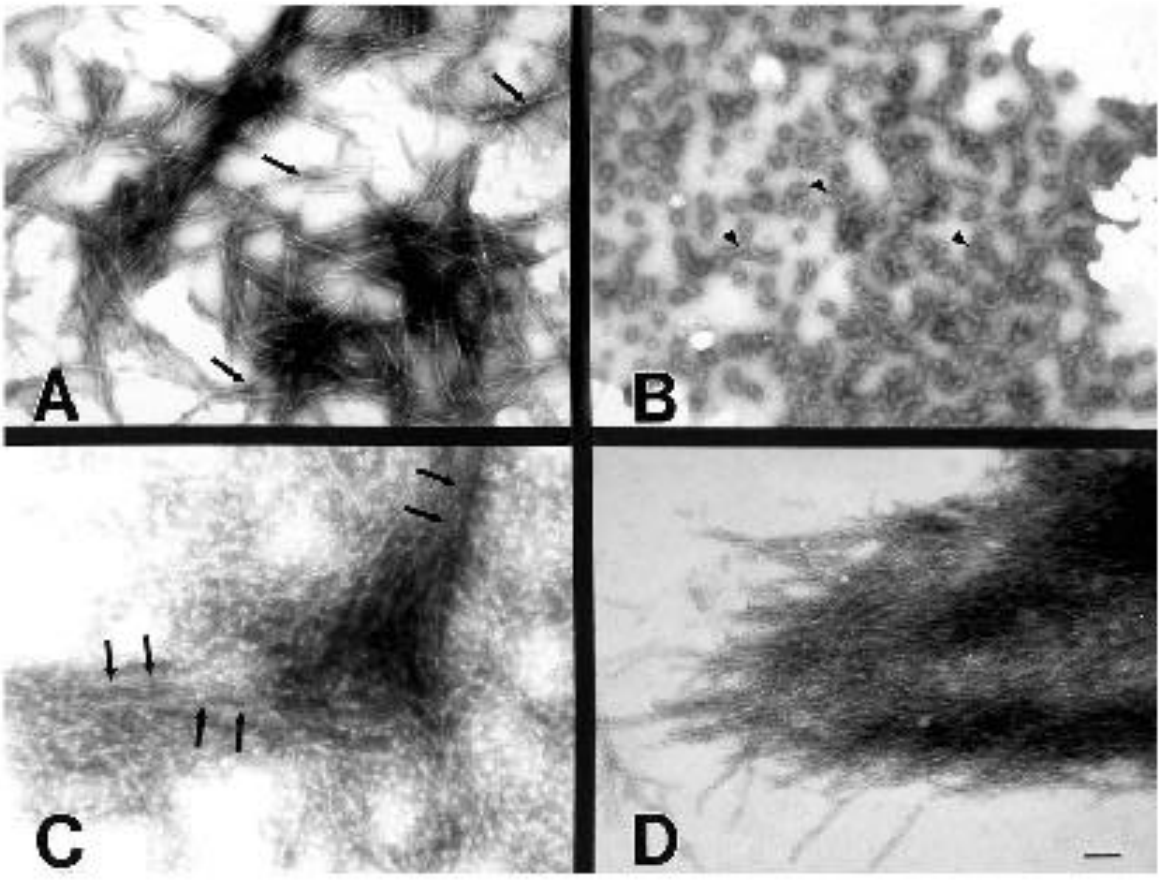

FIG. 6. Compaction of amylin fibrils by perlecan and perlecan GAGs as revealed by negative stain electron microscopy. Negative stain electron microscopy of 1-h incubation mixtures containing amylin only (*A*), perlecan only (*B*), amylin plus perlecan (*C*), or amylin plus heparin (*D*). *A*: Amylin alone demonstrated fibrils (*arrows*) of 7–10 nm in diameter, in an irregular array. *B*: Perlecan alone demonstrated coalescing globular structures (*arrows*) indicative of perlecan's globular domains. *C*: Perlecan plus amylin resulted in a general compaction of amylin fibrils. Tracks of lateral amylin fibrils (*arrows*) are observed intermingled with perlecan globular structures. *D*: A similar aggregation of amylin fibrils is observed when amylin is incubated in the presence of heparin. All photomicrographs are of the same magnification; bar in *D* = 100 nm.

observations suggest that amyloidogenic sequences are necessary but not sufficient to cause amylin amyloidosis in the pancreas. In addition, overexpression of human amylin in transgenic mice does not always lead to pancreatic amyloidosis (43,44). Therefore amylin deposition and decreased degradation may be responsible for islet amyloidosis. The extracellular matrix location of perlecan and its ability to bind amylin may contribute to islet amyloid deposition. Whether perlecan also inhibits amylin degradation once bound is a subject for future investigation. However, in other amyloidoses, such as the Aβ of Alzheimer's disease, perlecan once bound protects the Aβ amyloid from protease degradation (45).

Results from previous studies have suggested that the toxicity effects of human amylin are related to its fibrillar nature (7,35), since nonfibrillar rat amylin is not toxic to cells. The fibrillogenic region of human amylin is located at residues 20–29 (35,46–48), as rat amylin with specific proline substitutions within this domain negates the formation of a β-pleated sheet structure characteristic of amyloid. Although human amylin 20–29 can form fibrils (35), it is not toxic (7). This is consistent with the mechanism whereby amylin 20–29, which lacks basic residues (such as those present at positions 1 and 11 of amylin 1–37), will be predicted not to bind perlecan and therefore will not be deposited. By virtue of perlecan's ability to bind full-length amylin and enhance amylin fibril formation, the results of the present study also suggest that perlecan may play an important pathogenic role by contributing to the eventual toxicity that is observed in the pancreatic β-cells of type 2 diabetic patients. The retention of amylin (i.e., deposition and persistence) in the matrix may be necessary for the presentation of toxic amylin fibrils to the islet cells. Previous studies have demonstrated that the toxicity of the Aβ in Alzheimer's disease can be alleviated by treating cultures with soluble sulfated GAGs (49,50). Because perlecan also co-accumulates with Aβ in the brain of Alzheimer's disease patients (14,15), it is likely that the mechanism for the observed reduced toxicity involves the competitive inhibition of Aβ fibril interactions to cell or matrix-associated proteoglycans by soluble GAGs. A similar contribution of perlecan to the toxicity of islet amyloid may occur by virtue of amylin's interaction with matrix-bound perlecan during islet amyloidosis.

Perlecan interaction and enhancement of fibril formation also occurs with the Alzheimer's disease Aβ. Besides

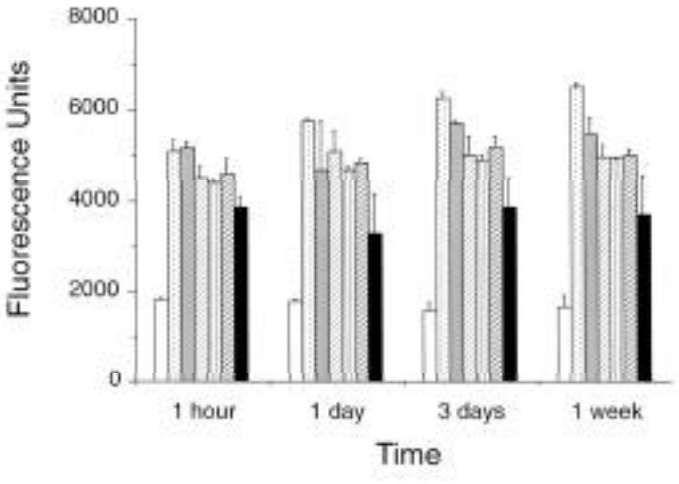

FIG. 7. Enhancement of amylin fibril formation by other sulfated GAGs and related macromolecules. Amylin (25 µmol/l) was incubated at 37°C for 1 week alone (□) or in the presence of 100 µl/ml each of heparin (~5 kDa) (▩), heparan sulfate from kidney (~12 kDa) (▩), chondroitin-4-sulfate (~30 kDa) (▨), dermatan sulfate (~16 kDa) (▥), dextran sulfate (~8 kDa) (▩), or pentosan polysulfate (~3 kDa) (■). Aliquots (50 µl) were taken for thioflavin T fluorometry analysis at 1 h, 1 day, 3 days, and 1 week. During the 1-week incubation period, the amount of amylin fibrils remained relatively constant. On a per weight basis, heparin and heparan sulfate GAGs were the most effective enhancers of amylin fibril formation, followed by chondroitin-4-sulfate, dermatan sulfate, and dextran sulfate. Pentosan polysulfate was the least effective, even though it increased amylin fibril formation approximately twofold within 1 h of incubation.

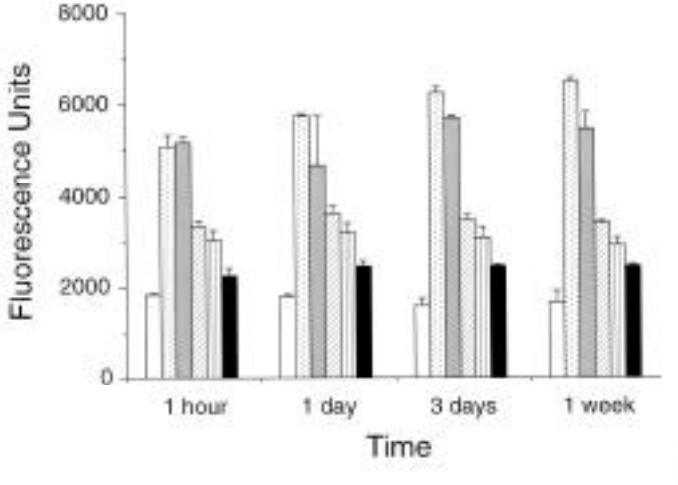

FIG. 8. Effects of heparin structural modifications on amylin fibril formation. Amylin (25 µmol/l) was incubated at 37°C for 1 week alone (□) or in the presence of 100 µg/ml of heparin (▩), heparan sulfate from kidney (▩), *N*-desulfated *N*-acetylated heparin (▨), completely desulfated *N*-sulfated heparin (▥), or completely desulfated *N*-acetylated heparin (■). Aliquots (50 µl) were taken for thioflavin T fluorometry analysis at 1 h, 1 day, 3 days, and 1 week. During the 1-week incubation period, the amount of amylin fibrils remained relatively constant in the absence of GAGs or modified GAG derivatives. A progressive loss of the stimulatory effect of heparin on amylin fibril formation was observed with the removal of sulfates along the GAG chains such that *N*-desulfation *N*-acetylation > complete desulfation *N*-sulfation > complete desulfation *N*-acetylation. Removal of all sulfates (i.e., complete desulfation *N*-acetylation) of heparin led to a significant ($P < 0.005$) 86.3% loss of the enhancement effect on amylin fibril formation.

the known association of perlecan with islet amyloid (11), perlecan appears to be an invariable proteoglycan that is found in association with a variety of amyloids, independent of the nature of the amyloid protein deposited and the extent of amyloid deposition (14). Similar to the findings in the present study regarding perlecan's effects on amylin fibril formation, recent studies have also indicated that perlecan not only binds to the predominant Aβ isoforms (i.e., Aβ 1–42 and Aβ 1–40) of Alzheimer's disease but also accelerates Aβ (1–40) fibril formation (23,24). The perlecan interaction with Aβ was also found to be primarily mediated by perlecan's GAG chains, which confirms a pivotal role for perlecan in the pathogenesis of Aβ amyloidosis in Alzheimer's disease. Preliminary data (51) have suggested that the perlecan GAG interaction with Aβ is due to both sulfate content and specific GAG backbone structure, as observed in the present investigation. The similarities of binding interaction and acceleration of fibril formation by perlecan for both Aβ and amylin indicate that perlecan likely plays a similar role in amyloidosis, regardless of the nature of the specific amyloid protein involved. These findings also suggest that therapeutic interventions for one type of amyloid involving perlecan and/or other proteoglycans may likely be effective for a variety of different amyloids.

ACKNOWLEDGMENTS

This work was supported in part by National Institutes of Health Grants AG-05136 and AG-12953 (A.D.S.) and a grant from Novo Nordisk A/S.

REFERENCES

1. Westermark P, Wernstedt C, O'Brien TD, Hayden DW, Johnson KH: Islet amy-

TABLE 1
Carbohydrate backbone composition and average sulfate content of GAGs and related macromolecules used in present study

GAG/sulfated macromolecules	Repeating units	Average sulfate content per repeating unit (reference)
Heparin	Glucosamine 1→4 glucuronic/iduronic acid	2.4 (38,40)
Heparan sulfate	Glucosamine 1→4 glucuronic/iduronic acid	0.5–0.9 (38,40)
Chondroitin 4-sulfate	Galactosamine 1→4 glucuronic acid	1.0 (41)
Dermatan sulfate	Galactosamine 1→4 glucuronic/iduronic acid	1.2 (40)
Dextran sulfate	Glucose 1→6 glucose	3–4 (Sigma)
Pentosan Polysulfate	Xylose 1→4 xylose	3–4 (Sigma)

loid in type 2 human diabetes mellitus and adult diabetic cats contains a novel putative polypeptide hormone. *Am J Pathol* 127:414–417, 1987
2. Clark A, Chargé SB, Badman MK, de Koning EJ: Islet amyloid in type 2 (non-insulin-dependent) diabetes. *APMIS* 104:12–18, 1996
3. Cooper GJ, Willis AC, Clark A, Turner RC, Sim RB, Reid KB: Purification and characterization of a peptide from amyloid-rich pancreases of type 2 diabetic patients. *Proc Natl Acad Sci USA* 84:8628–8632, 1987
4. Kahn SE, D'Alessio DA, Schwartz MW, Fujimoto WY, Ensinck JW, Taborsky GJ-J, Porte D-J: Evidence of cosecretion of islet amyloid polypeptide and insulin by beta-cells. *Diabetes* 39:634–638, 1990
5. Clark A, Edwards CA, Ostle LR, Sutton R, Rothbard JB, Morris JF, Turner RC: Localisation of islet amyloid peptide in lipofuscin bodies and secretory granules of human B-cells and in islets of type-2 diabetic subjects. *Cell Tissue Res* 257:179–185, 1989
6. Lorenzo A, Razzaboni B, Weir GC, Yankner BA: Pancreatic islet cell toxicity of amylin associated with type-2 diabetes mellitus. *Nature* 368:756–760, 1994
7. May PC, Boggs LN, Fuson KS: Neurotoxicity of human amylin in rat primary hippocampal cultures: similarity to Alzheimer's disease amyloid-beta neurotoxicity. *J Neurochem* 61:2330–2333, 1993
8. Howard CF-J: Longitudinal studies on the development of diabetes in individual *Macaca nigra*. *Diabetologia* 29:301–306, 1986
9. Porte D Jr: Banting Lecture 1990: beta-cells in type 2 diabetes mellitus. *Diabetes* 40:166–180, 1991
10. O'Brien TD, Butler PC, Kreutter DK, Kane LA, Eberhardt NL: Human islet amyloid polypeptide expression in COS-1 cells: a model of intracellular amyloidogenesis. *Am J Pathol* 147:609–616, 1995
11. Young ID, Ailles L, Narindrasorasak S, Tan R, Kisilevsky R: Localization of the basement membrane heparan sulfate proteoglycan in islet amyloid deposits in type II diabetes mellitus. *Arch Pathol Lab Med* 116:951–954, 1992
12. Verchere CB, D'Alessio DA, Palmiter RD, Weir GC, Bonner-Weir S, Baskin DG, Kahn SE: Islet amyloid formation associated with hyperglycemia in transgenic mice with pancreatic beta cell expression of human islet amyloid polypeptide. *Proc Natl Acad Sci USA* 93:3492–3496, 1996
13. Verchere CB, D'Alessio DA, Palmiter RD, Baskin DG, Snow AD, Bonner-Weir S, Kahn SE: Characterization of islet amyloid in a transgenic mouse model of NIDDM. *Diabetes* 45 (Suppl. 2):313A, 1996
14. Snow AD, Wight TN: Proteoglycans in the pathogenesis of Alzheimer's disease and other amyloidoses (Review). *Neurobiol Aging* 10:481–497, 1989
15. Snow AD, Mar H, Nochlin D, Kimata K, Kato M, Suzuki S, Hassell J, Wight TN: The presence of heparan sulfate proteoglycans in the neuritic plaques and congophilic angiopathy in Alzheimer's disease. *Am J Pathol* 133:456–463, 1988
16. Snow AD, Mar H, Nochlin D, Sekiguchi RT, Kimata K, Koike Y, Wight TN: Early accumulation of heparan sulfate in neurons and in the beta-amyloid protein-containing lesions of Alzheimer's disease and Down's syndrome. *Am J Pathol* 137:1253–1270, 1990
17. Perlmutter L, Chui H, Saperia D, Athanikar J: Microangiopathy and the colocalization of heparan sulfate proteoglycan with amyloid in senile plaques of Alzheimer's disease. *Brain Res* 508:13–19, 1990
18. Su JH, Cummings BJ, Cotman CW: Localization of heparan sulfate glycosaminoglycan and proteoglycan core protein in aged brain and Alzheimer's disease. *Neuroscience* 51:801–813, 1992
19. Van-Gool D, David G, Lammens M, Baro F, Dom R: Heparan sulfate expression patterns in the amyloid deposits of patients with Alzheimer's and Lewy body type. *Dementia* 4:308–314, 1993
20. Snow AD, Wight TN, Nochlin D, Koike Y, Kimata K, DeArmond SJ, Prusiner SB: Immunolocalization of heparan sulfate proteoglycans to the prion protein amyloid plaques of Gerstmann-Straussler syndrome, Creutzfeldt-Jakob disease and scrapie. *Lab Invest* 63:601–611, 1990
21. Snow AD, Bramson R, Mar H, Wight TN, Kisilevsky R: A temporal and ultrastructural relationship between heparan sulfate proteoglycans and AA amyloid in experimental amyloidosis. *J Histochem Cytochem* 39:1321–1330, 1991
22. Castillo GM, Cummings JA, Ngo C, Yang W, Snow AD: Novel purification and detailed characterization of perlecan isolated from the Engelbreth-Holm-Swarm tumor for use in an animal model of Aβ amyloid persistance in brain. *J Biochem* 120:433–444, 1996
23. Castillo GM, Ngo CT, Snow AD: Perlecan binding to Alzheimer's disease beta-amyloid protein (Aβ) 1–40 regardless of the extent of fibrillogenesis (Abstract). *Soc Neurosci Abstr* 22:1172, 1996
24. Castillo GM, Ngo C, Cummings J, Wight TN, Snow AD: Perlecan binds to the β-amyloid proteins (Aβ) of Alzheimer's disease, accelerates Aβ fibril formation, and maintains Aβ fibril stability. *J Neurochem* 69:2452–2465, 1997
25. Castillo GM, Templeton DM: Structure and metabolism of multiple heparan sulphate proteoglycans synthesized by the isolated rat glomerulus. *Biochim Biophys Acta* 1136:119–128, 1992
26. Björnsson S: Simultaneous preparation and quantitation of proteoglycans by precipitation with Alcian blue. *Anal Biochem* 210:282–291, 1993
27. Levine H III: Thioflavine T interaction with synthetic Alzheimer's disease beta-amyloid peptides: detection of amyloid aggregation in solution. *Protein Sci* 2:404–410, 1993
28. Levine H III: Thioflavin T interaction with amyloid beta-sheet structures. *Amyloid: Int J Exp Clin Invest* 2:1–6, 1995
29. Naiki H, Higuchi K, Nakakuki K, Takeda T: Kinetic analysis of amyloid fibril polymerization in vitro. *Lab Invest* 65:104–110, 1991
30. Naiki H, Nakakuki K: First-order kinetic model of Alzheimer's beta-amyloid fibril extension in vitro. *Lab Invest* 74:374–383, 1996
31. Puchtler H, Sweat F, Levine M: On the binding of Congo red by amyloid. *J Histochem Cytochem* 10:355–364, 1962
32. Engel J, Schalch W: Antibody binding constants from Farr test and other radioimmunoassays: a theoretical and experimental analysis. *Mol Immunol* 17:675–680, 1980
33. Mann K, Deutzmann R, Timpl R: Characterization of proteolytic fragments of the laminin-nidogen complex and their activity in ligand-binding assays. *Eur J Biochem* 178:71–80, 1988
34. Fox JW, Mayer U, Nischt R, Aumailley M, Reinhardt D, Wiedemann H, Mann K, Timpl R, Krieg T, Engel J, Chui ML: Recombinant nidogen consists of three globular domains and mediates binding of laminin to collagen type IV. *EMBO J* 10:3137–3146, 1991
35. Westermark P, Engstrom U, Johnson KH, Westermark GT, Betsholtz C: Islet amyloid polypeptide: pinpointing amino acid residues linked to amyloid fibril formation. *Proc Natl Acad Sci USA* 87:5036–5040, 1990
36. Guo YC, Conrad HE: The disaccharide composition of heparins and heparan sulfates. *Anal Biochem* 176:96–104, 1989
37. Chargé SB, de Koning EJ, Clark A: Effect of pH and insulin on fibrillogenesis of islet amyloid polypeptide in vitro. *Biochemistry* 34:14588–14593, 1995
38. Höök M, Lindahl U, Iverrius PH: Distribution of sulphate and iduronic acid residues in heparin and heparan sulphate. *Biochem J* 137:33–43, 1974
39. Fransson LA, Malmström A, Sjöberg I: Periodate oxidation and alkaline degradation of heparin related glycans. *Carbohydr Res* 80:131–145, 1980
40. Yanagishita M, Hascall VC: Characterization of heparan sulfate proteoglycans synthesized by rat ovarian granulosa cells in culture. *J Biol Chem* 258:12857–12864, 1983
41. Comper WD: Extracellular matrix interactions: sulfation of connective tissue polysaccharides creates macroion binding templates and conditions for dissipative structure formation. *J Theor Biol* 145:497–509, 1990
42. Jordan K, Murtaugh MP, O'Brien TD, Westermark P, Betsholtz C, Johnson KH: Canine IAPP cDNA sequence provides important clues regarding diabetogenesis and amyloidogenesis in type 2 diabetes. *Biochem Biophys Res Commun* 169:502–508, 1990
43. Höppener JW, Oosterwijk C, van Hulst KL, Verbeek JS, Capel PJ, de Koning EJ, Clark A, Jansz HS, Lips CJ: Molecular physiology of the islet amyloid polypeptide (IAPP)/amylin gene in man, rat, and transgenic mice. *J Cell Biochem* 55 (Suppl.):39–53, 1994
44. D'Alessio DA, Verchere CB, Kahn SE, Hoagland V, Baskin DG, Palmiter RD, Ensinck JW: Pancreatic expression and secretion of human islet amyloid polypeptide in a transgenic mouse. *Diabetes* 43:1457–1461, 1994
45. Gupta-Bansal R, Frederickson RC, Brunden KR: Proteoglycan-mediated inhibition of abeta proteolysis: a potential cause of senile plaque accumulation. *J Biol Chem* 270:18666–18671, 1995
46. Asai J, Nakazato M, Kangawa K, Matsukura S, Matsuo H: Isolation and sequence determination of rat islet amyloid polypeptide. *Biochem Biophys Res Commun* 164:400–405, 1989
47. Balasubramaniam A, Renugopalakrishnan V, Stein M, Fischer JE, Chance WT: Syntheses, structures and anorectic effects of human and rat amylin. *Peptides* 12:919–924, 1991
48. McLean LR, Balasubramaniam A: Promotion of beta-structure by interaction of diabetes associated polypeptide (amylin) with phosphatidylcholine. *Biochim Biophys Acta* 1122:317–320, 1992
49. Woods AG, Cribbs DH, Whittemore ER, Cotman CW: Heparan sulfate and chondroitin sulfate glycosaminoglycan attenuate beta-amyloid(25–35) induced neurodegeneration in cultured hippocampal neurons. *Brain Res* 697:53–62, 1995
50. Pollack SJ, Sadler II, Hawtin SR, Tailor VJ, Shearman MS: Sulfated glycosaminoglycans and dyes attenuate the neurotoxic effects of beta-amyloid in rat PC12 cells. *Neurosci Lett* 184:113–116, 1995
51. Castillo GM, Lukito W, Nochlin D, Ngo C, Snow AD: The glycosaminoglycans of perlecan bind beta-amyloid protein (Aβ) and enhance Aβ fibril formation in a sulfate content dependent manner (Abstract). *Soc Neurosci Abstr* 23:1882, 1997

Author Queries (please see Q in margin and underlined text)

Q1: Correct now?
Q1A: Is K_d defined correctly as “dissociation constant” and please define M_r.
Q2: TBS correctly spelled out?>
Q3: Name and city/state or city/country of manufacturer?>
Q4: Name and city/state or city/country of microscope?>
Q5: City?>
Q6: Please specify to what “its” refers.>
Q6a: Bar is given as “100 nm in D, Figure 6, and in Figure 5, page 6, bar is given as “100 µm.” Ok as is?
Q7: Rewording okay?>
Q8: Addition correct?>
Ref. 2 and 37: Should Charg’e be Chargé?>
Ref 2: Last name of de KEJ?>
Ref. 23: Are these proceedings or a journal? If the latter, please give publisher name and location and any editors, if applicable.>
Ref. 34: Word “nidogen” correct?>
Ref 43: Part of last name missing with “van” and “de”?
Ref 43: Supplement number?>
Ref 51: Please give full journal title and full page range.>